Deformation Pattern Modifications Induced by 2021 Brentonico Earthquake: Insights from EGMS Ortho Products

Rasoul Eskandari [1], Nicola Genzano [1], Marco Scaioni [1]

[1] Department of Architecture, Built Environment and Construction Engineering, Politecnico di Milano
via Ponzio 31, 20133 Milano, Italy {rasoul.eskandari, nicola.genzano, marco.scaioni}@polimi.it

Keywords: Earthquake, EGMS, Ground deformation, InSAR, Pattern Modification, Post-seismic

Abstract

Post-seismic deformation reflects the crustal adjustment to stress perturbations induced by earthquakes and may lead to modifications of ongoing deformation patterns. While such effects are well documented for moderate-to-large events, their detectability and significance after low-magnitude earthquakes remain poorly understood. Here, possible deformation pattern modifications associated with the February 2022 ML 3.5 Brentonico earthquake in Northearn Italy are investigated using ground-deformation time series derived from the European Ground Motion Service (EGMS) Ortho products. The earthquake occurrence is treated as a temporal discontinuity, enabling the estimation of pre- and post-event vertical/horizontal differential velocities during 2019-2023. A dual-weighted interpolation scheme, accounting for both spatial proximity and time-series reliability, is applied to derive spatially coherent maps of kinematic modifications. The results reveal measurable and spatially organized changes in deformation patterns, including localized accelerations/decelerations and direction reversals. A clear spatial correspondence between differential velocity anomalies and mapped fault systems suggests that the earthquake acted as a localized stress perturbation, modulating pre-existing tectonic structures. This study demonstrates the capability of EGMS datasets to capture post-seismic deformation signals and highlights the importance of considering low-magnitude events in long-term deformation analyses.

1. Introduction

Post-seismic deformation represents the transient adjustment of the Earth crust to the stress changes induced by an earthquake (Wimpenny et al., 2017), and can persist from days to years after the mainshock. It reflects a complex combination of mechanisms, typically including afterslip on and around the ruptured fault, viscoelastic relaxation in the lower crust and upper mantle, and poroelastic responses to coseismic fluid pressure changes (Diao et al., 2014; Nespoli et al., 2018). These processes can subtly modify pre-existing deformation patterns, either accelerating or damping ongoing motions, or even reversing local trends. Detecting such pattern modifications is essential to understand how faults and surrounding structures accommodate stress perturbations in time.

Among the techniques available to observe these changes, satellite Synthetic Aperture Radar Interferometry (InSAR) has become a key tool and allows systematic mapping of millimetre-scale ground motion over large regions. Numerous studies have used InSAR and Global Navigation Satellite System (GNSS) to investigate post-seismic deformation following moderate to large earthquakes, for example, in the Central Italy 2016 event (Pousse-Beltran et al., 2020), the Maduo event in China (Shu et al., 2024), the Kanto event in Japan (Elgharbawi and Tamura, 2015), and more recent sequences worldwide. These works show that post-seismic surface motions can be comparable in amplitude to the co-seismic signal and provide valuable constraints on fault friction, rheological structure and the relative importance of afterslip, viscoelastic and poroelastic contributions.

However, most case studies focus on large magnitude ($M_W \geq \sim 5$) events, while deformation changes associated with small earthquakes remain poorly explored. For such small events, expected surface signals are at the limit of detectability and can be easily masked by noise and non-tectonic trends, even though they may still perturb local stress fields or modulate ongoing deformation. Understanding how post-seismic deformation patterns evolve after small earthquakes is important for at least three reasons: it helps to (i) clarify the continuum between seismic and aseismic slip, (ii) identify structures that are mechanically coupled to the mainshock, and (iii) interpret long-term ground-motion products, where subtle trend changes may encode the cumulative effect of many small events.

In this work, possible deformation pattern modifications associated with the M_L 3.5 earthquake that occurred on 22nd February 2021 near Brentonico in Northern Italy have been investigated. Using the European Ground Motion Service (EGMS) Ortho vertical and horizontal (East-West) products from January 2019 to December 2023 (i.e., 3rd release), the earthquake origin time is considered as a turning point in the deformation time series (DefTS), and after a pre-processing stage, the subtle velocity variations across the pre- and post-event phases were calculated. By employing a dual-weighted interpolation framework, accounting for both spatial proximity and DefTS reliability, the localized kinematic anomalies are isolated and their correlation with the mapped fault systems is assessed.

This work suggests that even low-magnitude events may trigger measurable shifts in local ground deformation patterns, which may be often overlooked in standard seismic cycles. Besides the contribution of EGMS datasets for such anlyses, the findings offer insights into how pre-existing structures might modulate the long-term deformation response to localized stress perturbations.

2. Case study and material

As shown in Figure 1, the Area of Interest (AoI) for this study encompasses the southern sector of the Trentino-Alto Adige Italian region, specifically covering the northern basin of Garda Lake. This region is situated at the intersection of several major Alpine structural systems, making its surface kinematics highly sensitive to internal stress redistribution.

During the year 2021, two distinct seismic events were recorded within the boundaries of the AoI. The primary event, which is the

central focus of this investigation, occurred on 22 February 2021, with its epicenter located near Brentonico (TN). This earthquake was characterized as a local magnitude (M_L) 3.5 by the Istituto Nazionale di Geofisica e Vulcanologia (INGV), while the United States Geological Survey (USGS) earthquake catalog recorded it with a moment magnitude (M_W) of 4.3.
A second, lower-magnitude event was subsequently recorded on 17 November 2021, reaching a M_L3.0 according to the INGV. While both events are located within the study area, the February 22 earthquake is considered as the principal candidate for the observed kinematic shifts.

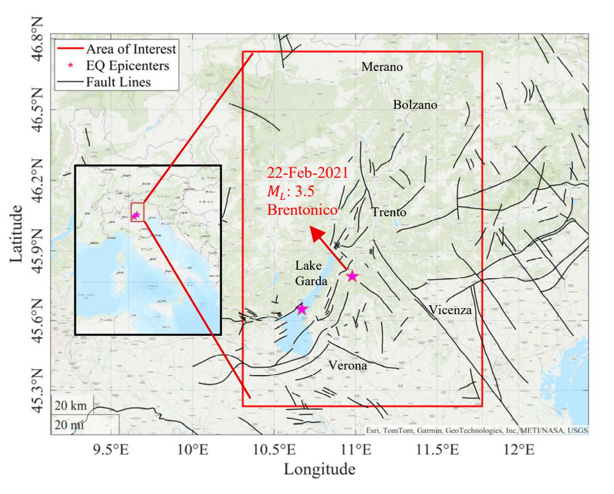

Figure 1. Area of February 2022 ML 3.5 Brentonico earthquake in Northearn Italy.

During the year 2021, two distinct seismic events were recorded within the boundaries of the AoI. The primary event, which is the central focus of this investigation, occurred on 22nd February 2021. The epicenter was located near Brentonico (TN). This earthquake was characterized as a local magnitude (M_L= 3.5) by the Istituto Nazionale di Geofisica e Vulcanologia (INGV), while the United States Geological Survey (USGS) earthquake catalog recorded it with a moment magnitude M_W=4.3.
A second, lower-magnitude event was subsequently recorded on 17th November 2021, reaching a M_L =3.0 according to the INGV. While both events were located within the study area, the February 22 earthquake is considered as the principal candidate for the observed kinematic shifts.
The analysis in this study is based on deformation time series (DefTS) provided by the European Ground Motion Service (EGMS) (https://egms.land.copernicus.eu/) . Operating as part of the Copernicus Land Monitoring Service (CLMS), the EGMS delivers validated displacement data derived from the multi-temporal interferometric processing of Sentinel-1 synthetic aperture radar (SAR) images. The service provides pan-European coverage with data available from January 2016, distributed through periodic releases that cover specific temporal windows (Crosetto et al., 2020; Costantini et al., 2022). EGMS products are categorized into three levels: L2A Basic, L2B Calibrated, and L3 Ortho. For this investigation, the L3 Ortho products were utilized. These products provide displacement components resampled onto a uniform 100-meter grid, decomposed into vertical Up-Down (U-D) and horizontal East-West (E-W) directions. It is important to note that due to the inherent geometric limitations of InSAR technology (specifically the near-polar orbit of the Sentinel-1 satellites), the sensitivity to deformation in the North-South is negligible. Consequently, this component is not provided by the service. The reliability of EGMS data has been demonstrated across diverse applications, including monitoring of critical infrastructure (Eskandari and Scaioni, 2023; Ruiz-Armenteros et al., 2025), landslide activity (Cuervas-Mons et al., 2024; Marmoni et al., 2025), land subsidence (Thiéblemont et al., 2024; Michalakis and Loupasakis, 2026), and regional tectonics (Eskandari et al., 2026).
In this study, six tiles from the third release of EGMS were exploited, covering the period from January 2019 to December 2023. This timeframe provides a robust baseline for evaluating the kinematic state of the AoI before and after the target seismic event. To correlate the observed deformation signals with the regional structural framework, fault lines were extracted from the ITHACA (ITaly HAzard from CApable faults) database (https://sgi.isprambiente.it/ithacaweb), provided by ISPRA Geological Survey of Italy. The fault lines are illustrated in Figure 1. This integration allows for a direct assessment of the role that pre-existing discontinuities played in modulating the post-seismic response.
Finally, to ensure the observed pattern modifications were not influenced by external environmental factors such as extreme rainfall or hydrological loading, precipitation time history for the Adige Valley was retrieved from the VisualCrossing (https://visualcrossing.com/) platform.

3. Methods

The primary objective of this study is to isolate and quantify the subtle kinematic modifications triggered by the February 2021 Brentonico earthquake, distinguishing them from long-term persistent trends and cyclic environmental noise. To achieve this, a multi-stage analytical framework is adopted, which is designed to treat the seismic event as a temporal discontinuity. To allow this, the method is structured into two primary stages: (1) the extraction and partial trend analysis of point-wise deformation data (Subsect. 3.1), followed by (2) the spatial interpolation of the resulting differential velocity fields (Subsect. 3.2).

3.1 Partial trend analysis

The initial stage involved the extraction of all measurement points (MPs) from the EGMS L3 Ortho products that fall within the AoI defined in Figure 1. This extraction was performed across the six exploited EGMS tiles to ensure a continuous dataset.
For both the vertical (U-D) and horizontal (E-W) components, the DefTS of each MP has undergone a pre-processing and de-seasoning procedure. To account for long-term non-linearities and seasonal fluctuations, a composite model consisting of a 3^{rd}order polynomial and a sinusoidal function was fitted to the entire temporal span (January 2019 to December 2023), as defined by:

$$D(t) = a_0 + a_1 t + a_2 t^2 + a_3 t^3 + \cdots + s_1 \sin(2\pi t) + s_2 \cos(2\pi t), \quad \text{(Eq. 1)}$$

where $D(t)$ represents the cumulative displacement at time t, $a_0, \ldots, a_3$ are the polynomial coefficients, and s_1 and s_2 represent the amplitudes of the annual periodic component. After estimating the model parameters via least-squares fitting, the root mean square error (RMSE) was calculated to assess fit quality and to be used in the subsequent steps. Then, the seasonal component, represented by the trigonometric terms in Equation 1, was subtracted from the original DefTS to isolate the underlying kinematic signal from periodic environmental noise.
Using the 22nd February 2021 earthquake as a temporal turning point, the de-seasoned DefTS were partitioned into pre-seismic and post-seismic phases. For each phase, a linear trend was

calculated to determine the mean velocities, denoted as V_{pre} and V_{pst}, respectively. This dual-phase evaluation was utilized to establish a baseline for the regional background kinematics and to identify any localized velocity fields potentially influenced by external factors.

To quantify the nature of the modification in the deformation process, the differential velocity ΔV was calculated using:

$$\Delta V = (V_{pst} - V_{pre}) \times sign(V_{pre}) \qquad \text{(Eq. 2)}$$

for each direction of deformation and per each MP. As defined by this formulation, the sign of ΔV provides a diagnostic measure of the kinematic shift. Positive values indicate an acceleration of the motion in the same direction as the pre-event trend, i.e., kinematic persistence. Conversely, negative values indicate a reduction in the magnitude of the pre-existing trend, i.e., a deceleration, or a complete reversal in the direction of movement.

3.2 Interpolation of differential velocities

When working with InSAR-derived DefTS (here, EGMS L3 Ortho data), a prudent treatment is required during the transition from point-wise estimates to spatial fields. Estimating linear trends from partitioned DefTS is particularly susceptible to unintended noise. If a mean velocity is noise-dominated, it can introduce significant bias into the ΔV calculation, as this measure is highly sensitive to the relative sign and magnitude of the pre- and post-seismic phases. To mitigate these potential biases and provide a spatially coherent representation of the kinematic alterations, the point-wise ΔV values were interpolated onto a uniform 500-m grid using a dual-weighted scheme. The interpolated differential velocity (ΔV_{int}) at each grid node is calculated according to:

$$\Delta V_{int} = \frac{\sum_{p=1}^{N} \omega_i^{dr} \cdot \Delta V_i}{\sum_{p=1}^{N} \omega_i^{dr}}, \qquad \text{(Eq. 3)}$$

where N represents the number of MPs within a 500-m radius of the interpolant node. The weights ω_i^{dr} are defined by a combined inverse-distance and inverse-error function, as shown in Equation 4,

$$\omega_i^{dr} = \left(\frac{1}{D_i}\right)^{\alpha_D} \cdot \left(\frac{1}{RSME_i}\right)^{\alpha_R}, \qquad \text{(Eq. 4)}$$

where D_i is the Euclidean distance from the i^{th} point to the interpolant node, and $RSME_i$ is the root mean square error derived from the initial trend fitting (see Subsect. 3.1), which serves as a proxy for the reliability of the DefTS. The exponents α_D and α_R control the influence of distance and error, respectively; in this study, both parameters are set to unity to establish a balanced dual-weighted interpolation.

By applying this inverse-distance, inverse-error weighting, a clearer representation of the wide-area ΔV fields is expected, effectively dampening the influence of unreliable or noisy MPs. The resulting interpolated fields were analyzed to identify post-seismic deformation pattern modifications across the AoI. Finally, these spatial signatures were examined in relation to the mapped fault systems to assess the correspondence between the observed kinematic regime changes and the underlying tectonic framework.

4. Results and discussion

4.1 Evidence in deformation time series

The first evidence of deformation pattern modification in the study area emerges from the deformation time series (DefTS). Several points exhibit different pre- and post-event behaviours, suggesting that the 22nd February 2021 Brentonico earthquake acted as a temporal turning point in the local deformation regime. This effect is visible in both vertical U-D and horizontal E-W components.

An example, extracted from a single EGMS L3 measurement point (MP), from the southern part of Bolzano is shown in Fig. 2, selected over area of interest (AoI). In the U-D component (Fig. 2a), the pre-event period shows a mild downward trend, while after the event the slope becomes clearly steeper towards more negative values, indicating an acceleration of ground lowering. In the E-W component (Fig. 2b), the pre-event signal is characterized by a significant westward trend, whereas after the event the DefTS flattens and then shows a slight eastward tendency. This indicates a strong reduction of the previous westward motion, locally evolving towards a deformation direction reversal.

These point-wise observations highlight a systematic shift in both vertical and horizontal velocity components. This temporal evidence of a kinematic regime change serves as the starting point for the spatial distribution analysis presented in the following subsections.

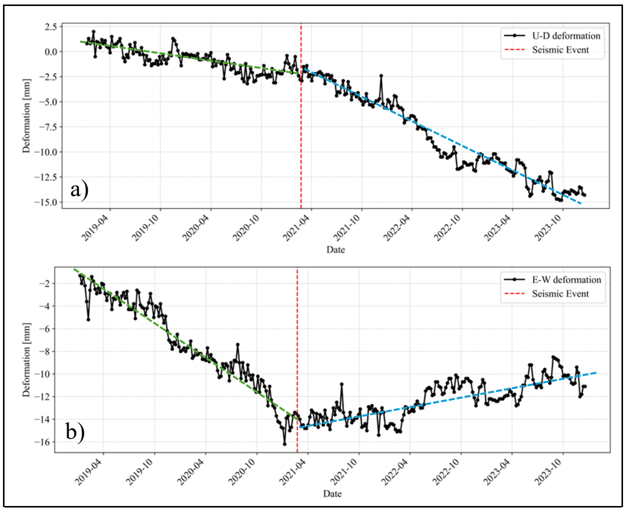

Figure 2. Example of deformation pattern modification in time domain: (a) Up-Down (U-D) and (b) East-West (E-W) deformation time series (source tile: EGMS-L3-E44N25, pid: 10VcAt6Eq6).

4.2 Pre- and post-event deformation fields

For transition from point-wise temporal observations to a regional perspective, the spatial distribution of ground velocities was analyzed across the AoI. Figures 3 and 4 illustrate the vertical (U-D) and horizontal (E-W) deformation velocities, respectively, comparing the pre-event (V_{pre}) and post-event (V_{pst}) phases as derived from the original EGMS L3 MPs.

On a regional scale, the global deformation pattern remains largely consistent across both periods. In the U-D component (Fig. 3), the north-western sector is characterized by a general uplift, while the southern portions of the AoI exhibit a steady subsidence trend. However, a closer inspection of the V_{pst} reveals significant localized deviations from the pre-seismic state. In the

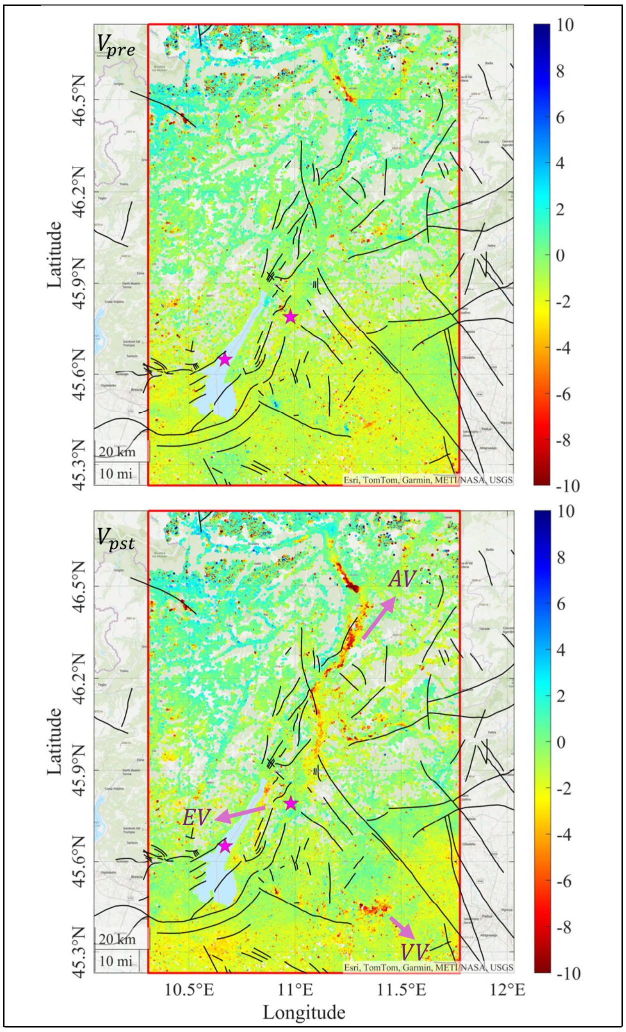

Figure 3. Pre- and post-seismic deformation velocities [mm/y] in U-D directions.

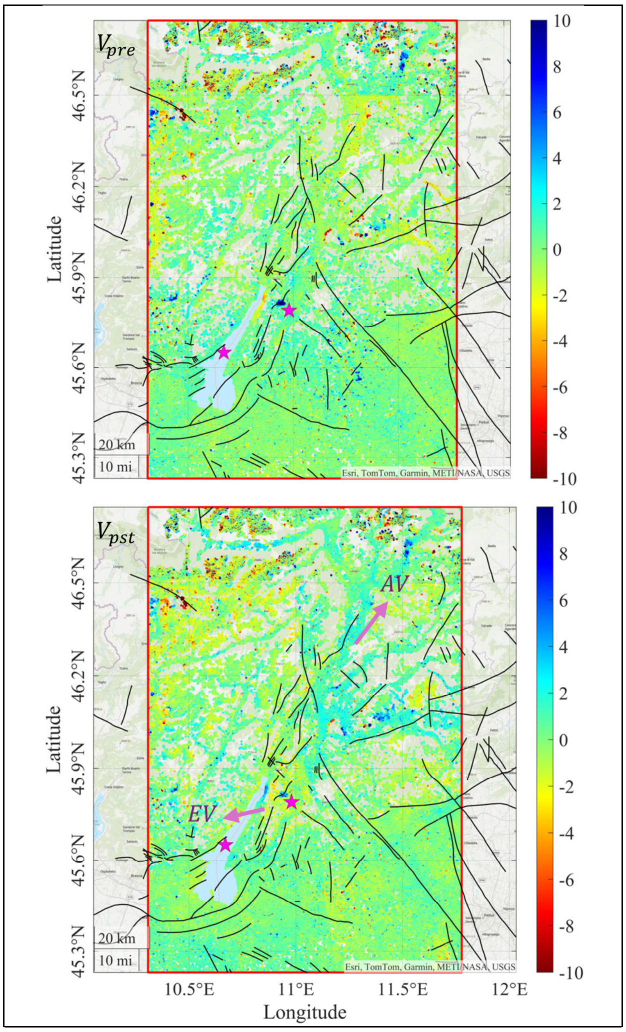

Figure 4. Pre- and post-seismic deformation velocities [mm/y] in E-W directions.

epicenter vicinity (EV), specifically a zone located at the north of Garda Lake, there is a distinct transition where previously uplifting zones shifted towards subsidence. Additionally, the zone between Verona and Vicenza (VV) shows a marked amplification of the existing subsidence rates. The most prominent modification is observed along the Adige Valley (AV), where a continuous belt of altered deformation behavior extends through Merano, Bolzano, Trento, and Rovereto towns.

A similar consistency in global kinematics, punctuated by localized post-seismic shifts, is evident in the E-W component (Fig. 4). Within the EV, the localized zone at the north of Garda Lake displays again a behavioral shift, while the area near Brentonico shows a notable deceleration in the rate of eastward deformation. Most significantly, the Adige Valley (AV) and its eastern flanks exhibit a pronounced eastwards movement in the post-seismic phase; a kinematic feature that was largely absent or negligible during the pre-event period.

By treating the February 2021 earthquake as a temporal turning point, it becomes evident that the regional-scale deformation remains largely consistent with the long-term baseline. Rather than a global shift, the possible impact of this seismic event is manifested as localized alterations, specifically concentrated within sectors of the AoI characterized by the high fault density and structural complexity.

4.3 Spatial distribution of differential velocities

As established in the previous subsections, the February 2021 seismic event did not trigger a uniform global shift in the regional kinematics; rather, its impact is concentrated within specific local sectors. To isolate these exposed zones and quantify the magnitude of the regime modifications, the spatial distribution of the interpolated differential velocities is analysed here, as shown in Figure 5.

The differential maps reinforce the observations from Subsection 4.2, while providing a clearer distinction between unaltered and modified zones. In the North-Western portion of the AoI, the signal appears as a noisy distribution of negligible-to-moderate variations. Conversely, over the southern sector, the U-D component shows a spatially smoothed representation of moderate modifications, while the E-W component reveals a subtle but widespread shift, confirming that the Southern basin responded more cohesively to the external trigger, possibly the seismic event.

The observable spatial correlation between local ΔV anomalies and several mapped fault systems suggests that the 2021 Brentonico earthquake acted as a structural trigger. The seismic energy likely redistributed stress along these pre-existing discontinuities (causing them to act as boundaries for the observed kinematic shifts), rather than inducing new fractures.

https://doi.org/10.5194/isprs-archives-XLIX-B3-2026-501-2026 | © Author(s) 2026. CC BY 4.0 License.

These anomalies are discussed separately for the U-D and E-W components in the following paragraphs.

4.3.1 Vertical (U-D) component

The vertical differential map (Fig. 5, U-D) highlights a significant trend reversal in the epicenter vicinity (EV). Specifically, the Northern zone of Garda Lake exhibits a localized rebound effect, shifting from pre-event subsidence to post-event uplift (negative ΔV). This suggests a localized stress release or a change in the compaction regime following the mainshock. Furthermore, a complex bidirectional behavior, characterized by adjacent zones of acceleration and deceleration, is evident along the Schio-Vicenza (SCV) normal fault (Castaldini and Panizza, 1991). This dipolar signature suggests a differential block response or tilting consistent with the NE-dipping nature of this normal fault system. However, the most high-magnitude, spatially correlated anomalies are concentrated along the Adige Valley. This signal originates near the Southern terminus of the Trento-Cles (TC) normal fault (Castaldini and Panizza, 1991) and extends toward Bolzano. The pattern reveals a distinct contrast: a significant acceleration of downward motion within the deep valley axis, flanked by deceleration along the lateral mountain ranges. This may point to fault-controlled sediment consolidation or a triggered adjustment of the valley-fill deposits.

4.3.2 Horizontal (E-W) component

The differential field (at the bottom of Fig. 5) is dominated by localized deceleration and kinematic reversals, where two distinct behaviors are observed: the magnitude decay and direction reversal. For example, along the Monte Altissimo di Nago (MAN) thrust fault (Castaldini and Panizza, 1991), there is a clear reduction in the pre-existing westwards velocity, indicated by a negative ΔV (red-to-yellow transition), which is related to the magnitude decay. This suggests that the thrust system may have experienced a temporary locking or a redistribution of strain that inhibited the prior motion. Regarding the direction reversal, a systematic eastwards shift is observed North of Lake Garda and across the entire AV and its Eastern flanks. This shift represents a fundamental change in the horizontal kinematic regime, where the regional westwards movement was superseded by an Eastwards adjustment in the post-seismic phase.

4.4 The Case of Paganella Fault

A particularly distinguished example of fault-modulated modification of deformation is observed along the Paganella (PGN) fault (Galadini and Galli, 1999), an ESE-dipping normal fault that defines the North-Western margin of the Adige Valley, as shown in Figure 5.

In the vertical U-D domain, the PGN fault acts as a sharp kinematic belt that aligns remarkably well with its structural characterization as an ESE-dipping normal fault. The hanging wall, located within the deep AV to the East of the fault trace, displays a prominent positive anomaly. Under ΔV logic, this signifies a marked acceleration of the pre-existing subsidence trend. This is a signature of normal faulting where the hanging wall block drops relative to the footwall in response to the extensional stress.

Conversely, the Western footwall represents a negative anomaly, indicating a reversal from pre-seismic uplift to post-seismic subsidence. This combined behavior, where the downwards movement of the valley floor intensifies while the adjacent mountain flank loses its upwards momentum and begins to sink, suggests a localized extensional unfolding or relaxation of the block. The February 2021 Brentonico earthquake likely acted as a trigger that reduced the effective stress on the ESE-dipping fault plane, allowing for a gravitational adjustment. In this case, the hanging wall slipped further into the basin, while the edge of the footwall experienced a downward flexural response as the structural support of the valley floor was weakened.

The horizontal E-W component reinforces this structural interpretation. Both sides of the PGN fault exhibit a negative differential signal. Given the pre-seismic Westward motion, it represents a widespread directional reversal towards East. The spatial coincidence of these kinematic breaks with the mapped trace of the PGN fault identifies it as a primary structural channel for post-seismic stress redistribution. This may suggest that the PGN fault system is not merely a passive feature but a reflexive boundary that actively partitions the regional strain in response to local seismic triggers.

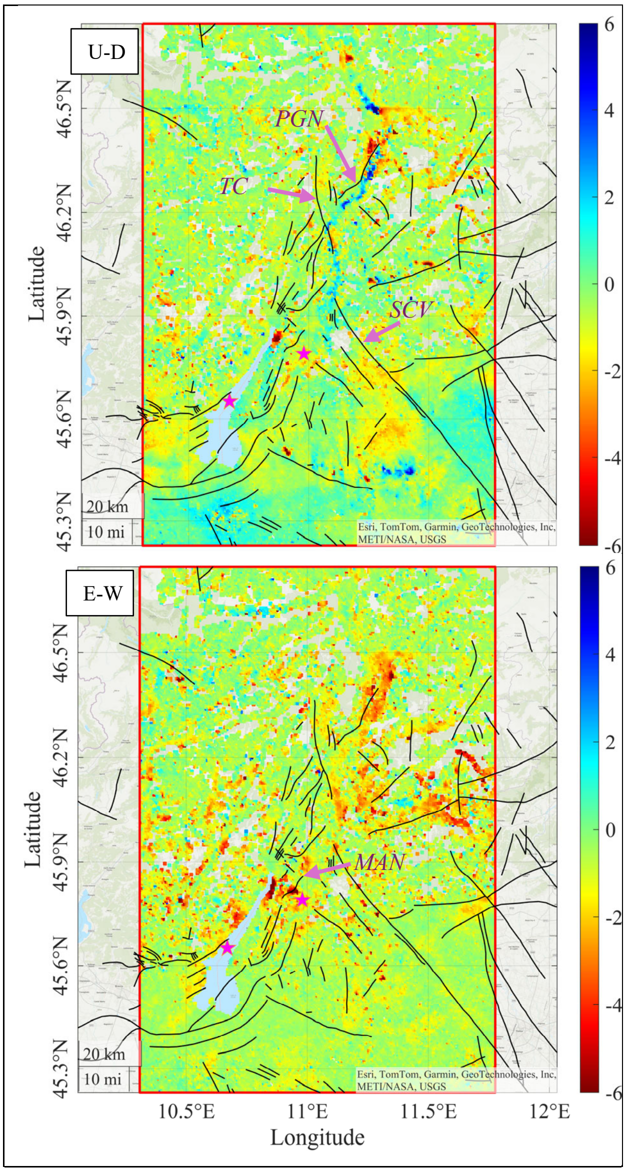

Figure 5. Interpolated differential velocity ΔV maps [mm/y] in U-D and E-W directions, and the fault system: *MAN* (Monte Altissimo di Nago fault), *PGN* (Paganella fault), *SCV*)Schio-Vicenza fault), and *TC* (Trento-Cles fault).

4.5 Evaluation of Non-Tectonic Factors

To ensure that the localized kinematic modifications identified in the previous subsections are indeed linked to the Febuary 2021 Brentonico earthquake, it is necessary to evaluate the influence of the secondary environmental forcing factors. In the Alpine context, ground deformation patterns are often sensitive to the hydrological loading and climatological cycles, particularly in deep valley systems such as the Adige Valley.

Figure 6 presents the daily and 7-day moving average precipitation distribution in the Adige Valley for the period spanning from January 2019 to December 2023 (the same period as DefTS of EGMS L3 used in this study). A critical analysis of this record reveals no significant climatological anomalies or extreme rainfall events in the immediate timeframe surrounding February 2021. While the valley experienced characteristic seasonal peaks (notably in late 2020 and late 2023), the specific turning point observed in the InSAR-derived DefTS (Fig. 2) coincides more with the seismic event and is likely tectonic rather a rainfall-induced surge and a response to pore-pressure changes from extreme precipitation. For a discussion on the specific type of surface response to extreme meteorological trigerring, interested readers may refer to Eskandari and Scaioni (2024; 2025).

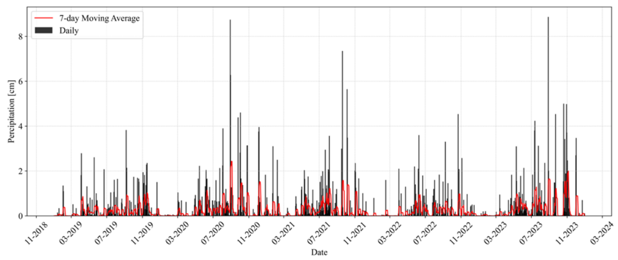

Figure 6. Distribution of precipitation in Adige Valley.

Nevertheless, a fully comprehensive robustness check would ideally incorporate additional environmental datasets, such as groundwater table fluctuations and snowmelt-induced loading models. While such variables could provide a higher degree of granularity in separating tectonic signals from anthropogenic or seasonal noise, their detailed investigation is beyond the current scope of this study.

Beyond climatological considerations, the technical consistency of the geospatial data was also evaluated. Although this study exploited six independent EGMS Ortho tiles, which are inherently generated through the resampling and decomposition of underlying L2B Calibrated products (through several smaller tiles), no evidence of systematic boundary-related errors or processing artifacts was detected in the spatial results. The identified kinematic patterns consistently align with major geomorphological and structural features, most notably the Adige Valley belt, reinforcing the interpretation that the detected signals represent authentic physical phenomena rather than product-level artifacts.

5. Conclusions

This study investigated the potential impact of the 22nd February 2021 Brentonico earthquake (ML=3.5) on regional deformation patterns using EGMS L3 Ortho deformation time series (DefTS). By treating the earthquake as a temporal discontinuity, a dual-phase analysis of pre- and post-event velocities was performed, enabling the quantification of kinematic modifications across the study area.

The results demonstrate that, despite the relatively low magnitude of the seismic event, measurable changes in deformation behaviour can be identified. The kinematic signatures extracted from the example DefTS reveal a pronounced sensitivity to the 2021 event, characterized by subsidence acceleration in the vertical domain and velocity reversals in the horizontal components. At the regional scale, while the overall deformation regime remains consistent, the differential velocity analysis reveals that the impact of the event is spatially heterogeneous and concentrated in structurally-complex, local zones. A key outcome of this work is the observed spatial correspondence between differential velocity anomalies and mapped fault systems. This relationship suggests that the seismic event did not generate a uniform regional response. Instead, it acted as a localized stress perturbation, reactivating or modulating pre-existing tectonic structures. In particular, fault-controlled kinematic decoupling, such as those observed along the Adige Valley and the Paganella fault, indicate that these discontinuities play an active role in partitioning post-seismic deformation.

The evaluation of precipitation records indicates that no significant meteorological anomalies coincided with the observed deformation changes, strengthening the hypothesis that the observed modifications are tectonically driven. While the influence of ancillary environmental or anthropogenic variables remains a consideration, the temporal alignment with the seismic event points out to a primarily stress-induced response.

Furthuremore, this study highlights the capability of EGMS datasets to detect subtle deformation pattern modifications even for low-magnitude earthquakes, contributing to a more comprehensive understanding of the continuum between seismic and aseismic deformation processes. Future work will be dedicated to integrating additional environmental and anthropogenic datasets, such as groundwater variations, snow loading, and land-use changes, to further unravel tectonic signals from external forcing factors. This will enhance the robustness and reliability of attributing observed kinametic modifications to the seismic events, particularly in complex Alpine environments.

Acknowledgement

The research activities carried out in this manuscript are supported by project TNE23-00012, 'Green & Pink for Sustainable Education' (GPSEducation), funded by Sub-Measure T4 'Transnational Initiatives in Education', Investment 3.4 'University Teaching and Advanced Skills' of the National Recovery and Resilience Plan, Mission 4 'Education and Research', Component 1 'Strengthening the Offering of Education Services: From Nursery Schools to University', for the promotion and implementation of transnational educational initiatives (TNE). The project is funded by the European Union, NextGenerationEU (CUP D74G23000280006).

The authors would like to thank Copernicus Land Monitoring Service (CLMS) for providing ground deformation data through European Ground Motion Service (EGMS), and ISPRA Geological Survey of Italy for providing fault dataset through ITHACA (ITaly HAzard from CApable faulting).

References

Castaldini, D.,Panizza, M., 1991. Inventario delle faglie attive tra i fiumi po e piave e il lago di Como (italia settentrionale). *Il Quaternario*, 4, 333-410.

Costantini, M., Minati, F., Trillo, F., Ferretti, A., Passera, E., Rucci, A., Dehls, J., Larsen, Y., Marinkovic, P., Eineder, M., Brcic, R., Siegmund, R., Kotzerke, P., Kenyeres, A., Costantini, V., Proietti, S., Solari, L., Andersen, H. S., 2022. EGMS: Europe-wide ground motion monitoring based on full resolution InSAR processing of all Sentinel-1 acquisitions. In: Proc. of IEEE International Geoscience and Remote Sensing Symposium (IGARSS 2022), Kuala Lumpur, Malaysia, 5093-5096.

Crosetto, M., Solari, L., Balasis-Levinsen, J., Casagli, N., Frei, M., Oyen, A.,Moldestad, D. A., 2020. Ground deformation monitoring at continental scale: The European ground motion service. *The International Archives of Photogrammetry, Remote Sensing and Spatial Information Sciences*, XLIII-B3-2020, 293-298.

Cuervas-Mons, J., Domínguez-Cuesta, M. J.,Jiménez-Sánchez, M., 2024. Potential and limitations of the new European ground motion service in landslides at a local scale. *Applied Sciences*, 14(17), paper No., 7796.

Diao, F., Xiong, X., Wang, R., Zheng, Y., Walter, T. R., Weng, H.,Li, J., 2014. Overlapping post-seismic deformation processes: Afterslip and viscoelastic relaxation following the 2011 Mw 9.0 Tohoku (Japan) earthquake. *Geophysical Journal International*, 196(1), 218-229.

ElGharbawi, T.,Tamura, M., 2015. Coseismic and postseismic deformation estimation of the 2011 Tohoku earthquake in Kanto region, Japan, using InSAR time series analysis and GPS. *Remote Sensing of Environment*, 168, 374-387.

Eskandari, R.,Scaioni, M., 2023. European ground motion service for bridge monitroing: Temporal and thermal deformation cross-check using Cosmo-SkyMed InSAR. *International Archives of the Photogrammetry, Remote Sensing and Spatial Information Sciences*, Vol. XLVIII, Part 1/W2-2023, 1235-1241.

Eskandari, R.,Scaioni, M., 2024. Spatiotemporal pattern detection of ground deformations induced by extreme rainfall using InSAR EGMS: The case of Cortina d’ampezzo after Vaia storm. *ISPRS Annals of the Photogrammetry, Remote Sensing and Spatial Information Sciences*, Vol. X, Part 3-2024, 131-138.

Eskandari, R.,Scaioni, M., 2025. InSAR EGMS for wide-area assessment of extreme rainfall-related modifications of ground-deformation patterns: The case of Vaia rainstorm. In: E. Borgogno Mondino, P. Zamperlin (Eds.), *Geomatics for Green and Digital Transition*, Communications in Computer and Information Science, Vol. 2463, Springer Nature, Cham (Switzerland), Part 1, 46–60.

Eskandari, R., Biparvayekhiabani, S., Genzano, N., Castiglioni, C. A.,Scaioni, M., 2026. Spatiotemporal evaluation of pre-seismic deformation patterns: The case of northern Thessaly, Greece. *International Archives of the Photogrammetry, Remote Sensing and Spatial Information Sciences*, Vol. XLVIII, Part 4/W18-2025, 131-137.

Galadini, F.,Galli, P., 1999. The Holocene paleoearthquakes on the 1915 avezzano earthquake faults (central Italy): Implications for active tectonics in the central apennines. *Tectonophysics*, 308(1-2), 143-170.

Marmoni, G. M., Antonielli, B., Caprari, P., Di Renzo, M. E., Marini, R., Mastrantoni, G., Mazzanti, P., Patelli, D.,Bozzano, F., 2025. Semi-automatic ranking of landslide candidate areas at a regional scale using EGMS InSAR data for territorial planning and risk management. *Landslides*, 22(12), 4077-4095.

Michalakis, I.,Loupasakis, C., 2026. Land subsidence and earthquake-timed vertical offsets in the messara basin, crete: EGMS-based screening for the 2021 Mw 6.0 arkalochori earthquake. *Land*, 15(4), paper No. 545.

Nespoli, M., Belardinelli, M. E., Gualandi, A., Serpelloni, E., Bonafede, M.J.G., 2018. Poroelasticity and fluid flow modeling for the 2012 Emilia-Romagna earthquakes: Hints from GPS and InSAR data.*Geofluids*, 2018(1), paper No. 4160570.

Pousse-Beltran, L., Socquet, A., Benedetti, L., Doin, M.-P., Rizza, M.,D'Agostino, N., 2020. Localized afterslip at geometrical complexities revealed by InSAR after the 2016 central Italy seismic sequence. *Journal of Geophysical Research: Solid Earth*, 125(11), paper No. e2019JB019065.

Ruiz-Armenteros, A. M., Marchamalo-Sacristán, M., Lamas-Fenández, F., Á, H.-C., Fenández-Landa, A., Delgado-Blasco, J. M., González-Tejada, I., Lazecky, M., Bakon, M., Perissin, D., Corral, G., Mesa-Mingorance, J. L., García-Balboa, J. L., Pacheco, A. D. P., Papco, J., Granados, A., Granados, I.,Sousa, J. J., 2025. Integrated monitoring of dam deformation using InSAR techniques, in-situ data, and advanced modeling: A case study with the European ground motion service (EGMS). In: Proc. of IEEE International Geoscience and Remote Sensing Symposium (IGARSS 2025), Brisbane, Australia, 9405-9408.

Shu, C., Meng, Z., Wu, Q., Xiong, W., He, L., Zhang, X.,Xu, D., 2024. Coseismic and early postseismic deformation mechanism following the 2021 Mw 7.4 Maduo earthquake: Insights from satellite radar interferometry and GPS. *Remote Sensing*, 16(8), paper No. 1399.

Thiéblemont, R., Le Cozannet, G., Nicholls, R. J., Rohmer, J., Wöppelmann, G., Raucoules, D., de Michele, M., Toimil, A., Lincke, D., 2024. Assessing current coastal subsidence at continental scale: Insights from Europe using the European ground motion service. *Earth's Future*, 12(8), paper No. e2024EF004523.

Wimpenny, S., Copley, A.,Ingleby, T., 2017. Fault mechanics and post-seismic deformation at Bam, SE Iran. *Geophysical Journal International*, 209(2), 1018-1035.